Assessing runoff sensitivities to precipitation and temperature changes under global climate-change scenarios

Lei Chen, Jianxia Chang, Yimin Wang and Yuelu Zhu

ABSTRACT

An accurate grasp of the influence of precipitation and temperature changes on the variation in both the magnitude and temporal patterns of runoff is crucial to the prevention of floods and droughts. However, there is a general lack of understanding of the ways in which runoff sensitivities to precipitation and temperature changes are associated with the CMIP5 scenarios. This paper investigates the hydrological response to future climate change under CMIP5 RCP scenarios by using the VIC model and then quantitatively assesses runoff sensitivities to precipitation and temperature changes under different scenarios by using a set of simulations with the control variable method. The source region of the Yellow River (SRYR) is an ideal area to study this problem. The results demonstrated that the precipitation effect was the dominant element influencing runoff change (the degree of influence approaching 23%), followed by maximum temperature (approaching 12%). The weakest element was minimum temperature (approaching 3%), despite the fact that the increases in minimum temperature were higher than the increases in maximum temperature. The results also indicated that the degree of runoff sensitivity to precipitation and temperature changes was subject to changing external climatic conditions.

Key words | climatic change, control variable method, delta method, runoff sensitivities, source region of the Yellow River, VIC model

Lei Chen
Jianxia Chang (corresponding author)
Yimin Wang
State Key Laboratory Base of Eco-Hydraulics in Northwest Arid Region of China,
Xi'an University of Technology,
Xi'an 710048,
China
E-mail: *chxiang@xaut.edu.cn*

Yuelu Zhu
Institute of Water Conservancy and Ecological Engineering,
Nanchang Institute of Technology,
Nanchang, 330000,
China

INTRODUCTION

In recent years, a broad consensus has developed that the global hydrological cycle will be affected by future global climate change (Bates *et al.* 2008; Gosling & Arnell 2016; Zarch *et al.* 2017). Under the condition of limited water resources, an accurate understanding of the law of space-time change in water resources is indispensable to the establishment of an effective management mechanism and to develop policies to adapt to this environmental change. The use of different kinds of global climate model (GCM) scenarios is extremely useful for projecting trends of future global climate changes and for understanding a range of possible runoff changes (Dosio & Panitz 2016; Pourmokhtarian *et al.* 2017). However, there is a general lack of understanding of the ways in which precipitation and temperature changes influence runoff at spatial and temporal scales under climate change scenarios.

Climate change may change land surface forcing including precipitation, temperature and other climate variables and may further result in changes in runoff (Andrews *et al.* 2015). Currently, there are two methods used in research to determine the impact of climate change on runoff. One method is based on the concept of the climate elasticity of runoff, with results obtained directly from historical meteorological elements and runoff time series (Schaake 1990;

doi: 10.2166/nh.2018.192

Yang & Yang 2011; Brikowski 2015; Fan *et al.* 2017). Another more commonly used method is the hydrological modelling approach (Dibike & Coulibaly 2005; Immerzeel *et al.* 2010; Teklesadik *et al.* 2017). Since climate and hydrological phenomena are significantly different in their spatial scales, a physics-based distributed hydrological model has been recognized as extremely effective at identifying temporal and spatial variability in runoff at the river-basin scale (Bhatti *et al.* 2016; Gregoretti *et al.* 2016; Huziy & Sushama 2017). In this approach, climate input variables of interest, such as precipitation and temperature, can be considered separately, and hydrological processes and fluxes (such as runoff and evaporation) can be simulated under conditions of climate change and changes in other drivers. Therefore, this approach can also be used to study the sensitivity of runoff to climate change. Compared to assumed climate change scenarios, global climate models have a clear physical meaning, are more readily used by the scientific community and are suitable for the hydrological modelling approach.

Substantial research on assessing the sensitivity of runoff to precipitation and temperature changes is being carried out worldwide. Nijssen *et al.* (2001) focused on the problem of climate change in macro-scale river basins (including the Amazon, Amur, Mackenzie, Mekong, Mississippi, Severnaya Dvina, Yellow, and Yenisei Rivers) around the world and found that the annual mean runoff decreased whenever temperatures increased. Tang *et al.* (2012) evaluated runoff changes/sensitivity when temperatures increased in the Salmon River Basin; the results also show that temperature increases generally lead to a decrease in runoff. Rasouli *et al.* (2014) provided the linearly scaled meteorological forcing inputs necessary to study model sensitivity in climate change scenarios. Their results showed that runoff, peak runoff, and the timing of peak runoff clearly have a sensitivity to both warming and precipitation changes. Bosshard *et al.* (2014) assessed the impact of climate change on the hydrology of the Rhine basin by using the PREVAH hydrological model and utilizing regional climate model data. Their results suggested that temperature effects are of prime importance for the Alpine tributaries, while precipitation effects dominate in the lower portion of the Rhine basin.

However, to date, most of these studies are aimed at the average temperature (Chang & Jung 2010). Only a few works discuss the runoff sensitivities to changes in meteorological elements associated with the CMIP5 models of various global climate change scenarios, which may not be sufficient for reliable estimates of the influence of temperature on runoff. Runoff in the hydrological system is affected by the change in average temperature. In addition, the susceptibility of runoff to the maximum and minimum temperatures accounted for a fairly large proportion of impacts, especially in areas of high altitude and large temperature differences (Zhang *et al.* 2014). The scientific programs behind this work are in accordance with the traditional hydro-meteorological observations as well as global climate models, together with climate change and the physically based hydrological model. The goal of this study is to objectively and comprehensively investigate the sensitivity of runoff to precipitation and temperature changes by separating the possible impacts of meteorological elements under the different climate change scenarios.

Under the condition of global warming, temperatures in high-altitude areas increase considerably more than temperatures in low altitude areas. This scenario exacerbates climate change-related problems in the region (Li *et al.* 2017b). The Tibetan Plateau, a sensitive and vulnerable region to climate warming, is the world's highest plateau. Recently, the rate of temperature rise over the Tibetan Plateau, which has a cold plateau climate, has been much higher than that of the surrounding areas (Zhou & Huang 2012). This region is also called the 'water tower of Asia'. As the origin of many rivers in Asia, the Tibetan Plateau has the headwaters of several world-class rivers, such as the Indus River in South Asia; the Brahmaputra River, the Salween River, and the Mekong River in Southeast Asia; and the Yangtze River and the Yellow River in China.

In this study, the source region of the Yellow River (SRYR) is taken as the case study area. It is located in the northeastern Tibetan Plateau and covers only 15% of the whole Yellow River basin but contributes to more than one-third of the total runoff. In recent years, climate changes have taken place in the Yellow River Basin, which are expected to continue in the future, inevitably leading to the appearance of progressive complex changes in the water resources of the region (Gao *et al.* 2016; Ren *et al.* 2016; Qin *et al.* 2017). Most of the previous works focused on analyzing the hydrological process under changes in

the climate and land use, but few of them attempted to investigate the runoff sensitivity under the different climate-change scenarios.

Therefore, this paper seeks to address the aforementioned issues by pursuing the following objectives: (1) to investigate the hydrological response to future climate change by using the VIC model, (2) to quantitatively assess the sensitivities of runoff to precipitation and temperature changes under different climate scenarios by using a set of simulations with the control variable method, based on identifying the separate and interacting effects of changes in precipitation and temperature on runoff to find the most sensitive elements and seasons that influence runoff, and (3) to conduct a study on the influence of external climatic conditions on the degree of runoff sensitivities to precipitation and temperature changes, with a quantification of the range in variation.

STUDY REGION AND DATA

Study region

The study region SRYR is located in the northeast Tibetan Plateau (95.5–103.5°E and 32–36.5°N), with the Tangnaihai hydrological station as the control outlet of the basin. The region is located in central Eurasia and has a cold plateau climate (Figure 1). The region has an obvious northwest–southeast inclined terrain, with most of the area at an altitude of 3,000 m above sea level, and a large temperature

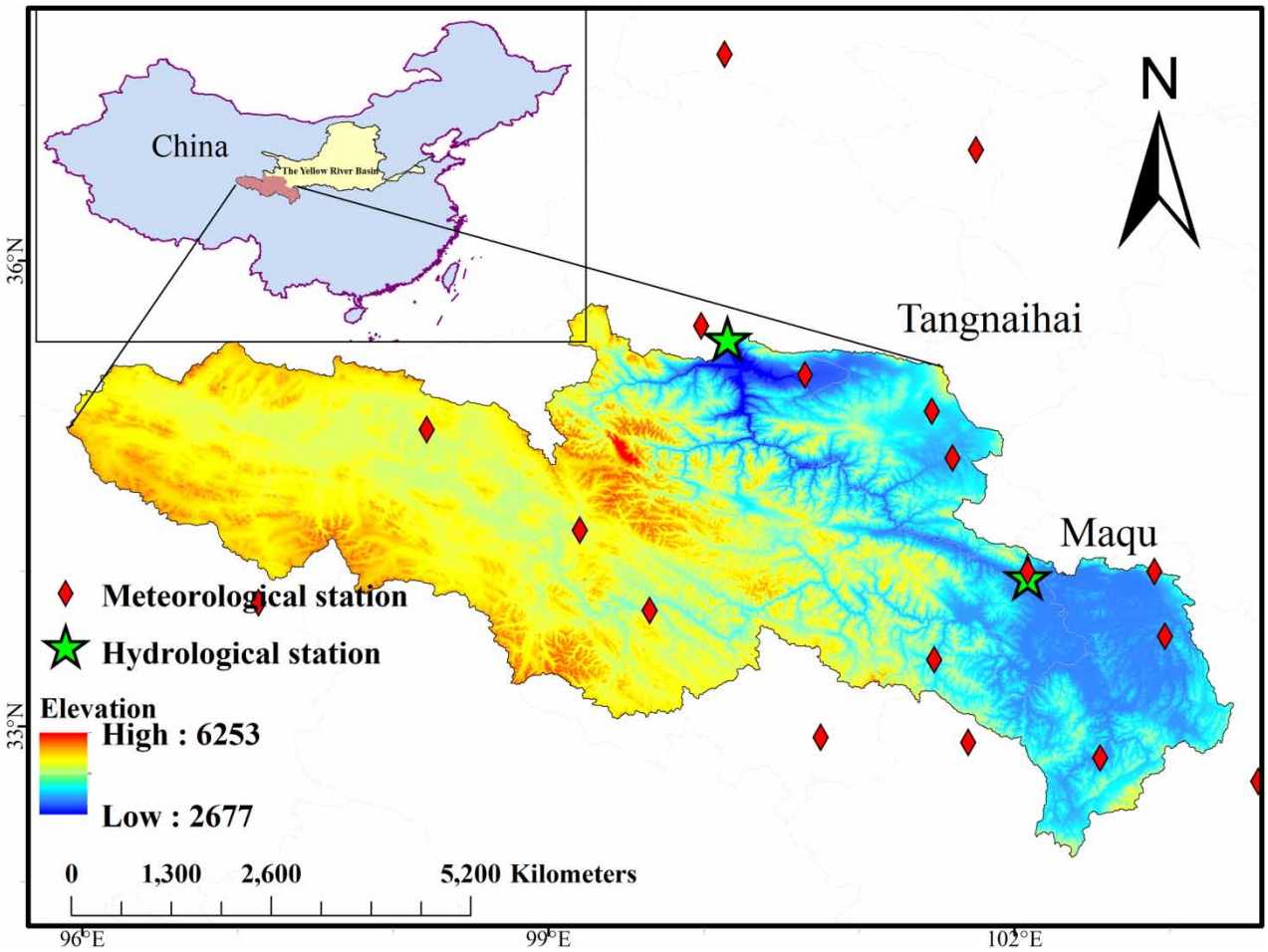

Figure 1 | Map of the SRYR and the location of hydrologic and metrological stations.

difference between day and night. The region serves as the source of the Yellow River and plays an important role in grain production and social development for the entire Yellow River region.

Data

A temporal and spatial sequence of meteorological elements and a spatial distribution of vegetation coverage and soil are necessary for most physically based hydrological models. The observations included meteorological data from 18 national basic weather stations in China, in and around the SRYR. These data cover the period from 1966 to 2005. The vegetation data were taken from 1-km global land-cover products provided by the University of Maryland. For soil parameters, information from the National Atmospheric and Oceanic Administration (NOAA) Hydrology Office soil classification was used.

In addition to the model input data, hydrological modelling was performed by comparing observed runoff to simulated runoff (Singh *et al.* 2017). The hydrological validation data included monthly natural runoff at hydrological stations, as calculated by the Yellow River Conservancy Committee (YRCC), located in the mainstem of the study area. The monthly natural runoff at two stations in the SRYR – the Maqu and Tangnaihai stations – were used for testing the performance of the VIC model.

METHODS AND MODELS

Climate models and scenarios

In different countries around the world, many GCMs have been developed and used. Each of these, forced by different emissions scenarios, will lead to a different prediction of climate change. In this study, the GCMs in phase 5 of the Coupled Model Intercomparison Project (CMIP5) under RCP4.5 and RCP8.5 scenarios were used for climate change projections. These three GCMs were BCC-CSM1.1 (*developed at the Beijing Climate Center, China Meteorological Administration*), MIROC-ESM and MIROC-ESM-CHEM (*both developed jointly by the Japan Agency for Marine-Earth Science and Technology, Atmosphere and Ocean Research Institute at the University of Tokyo, and National Institute for Environmental Studies*).

These GCMs divide the surface of the earth into 128 × 64 grid points with a horizontal resolution of T42, approximately the equivalent of a spatial grid size that is 2.8° latitude by 2.8° longitude. Predictor variable data were extracted from the GCMs for two time slices of the years 1966–2005 (due to the limited historical data by GCMs) and 2011–2050 for the RCP4.5 and RCP8.5 scenarios. The historical period 1966–2005 is defined as the baseline period. The spatial distribution for each meteorological element and runoff was based on the calibrated hydrological model by using the inverse distance weighted interpolation method in ArcGIS (10.2) platform.

Notably, to be prepared for the projections of future climate change, the first thing is to make sure the selected climate model is applicable to this region. Therefore, it is necessary to check the correlation between the GCMs outputs obtained through the downscaling method and meteorological observations in the baseline period of 1966–2005.

VIC hydrological model

In this study, the Variable Infiltration Capacity (VIC) model and an offline routing model were used together in a daily time step to simulate runoff. The VIC model (Liang *et al.* 1994) is a semi-distributed macroscale hydrological model, which has been successfully applied with practical results in many basins around the world (Bowling & Lettenmaier 2010; Mishra *et al.* 2011; Tatsumi & Yamashiki 2015). Moreover, the VIC model was introduced by many scholars and has been used to conduct extensive research in China (Liu *et al.* 2013; Ma *et al.* 2016; Huang *et al.* 2017). Among these studies, combining climate scenarios with VIC hydrological models is an important direction for research to generate an ensemble forecast for future possible variations in runoff under conditions of climate change (Zhai & Tao 2017).

The VIC model computation for runoff and base flow is executed on a grid cell in either a water balance or energy balance model, and the internal data of each grid cell are split into topographic elevation, multiple soil layers with variable infiltration rates, and multiple vegetation heterogeneity. The grid cell surface runoff by the VIC model was

summed downstream using a routing model that generated and transported to the outlet of that grid cell.

In practice, simple, effective and accurate models are required that assess the impact of climatic change on water resources regimes (Drogue *et al.* 2004). The objective of calibration and validation is to use as little information as accurately as possible to provide accurate hydrological models. To examine the VIC model performance for the calibration and validation periods, we used three statistical indices: the Nash–Sutcliffe efficiency (N_S; Nash & Sutcliffe 1970), the relative error ratio (E_r) and the correlation coefficient (R).

Nash–Sutcliffe efficiency (N_S):

$$N_s = 1 - \frac{\sum_{i=1}^{n} (Q_{nat,i} - Q_{sim,i})^2}{\sum_{i=1}^{n} (Q_{nat,i} - \overline{Q_{nat}})^2} \quad (1)$$

Relative error ratio (E_r):

$$E_r = \frac{|\overline{Q_{nat}} - \overline{Q_{sim}}|}{\overline{Q_{nat}}} \quad (2)$$

Correlation coefficient (R):

$$R = \frac{\sum_{i=1}^{n} (Q_{nat,i} - \overline{Q_{nat}})(Q_{sim,i} - \overline{Q_{sim}})}{\sqrt{\sum_{i=1}^{n} (Q_{nat,i} - \overline{Q_{nat}})^2 \sum_{i=1}^{n} (Q_{sim,i} - \overline{Q_{sim}})^2}} \quad (3)$$

where $Q_{nat,i}$ = natural runoff; $Q_{sim,I}$ = simulated runoff; $\overline{Q_{nat}}$ = mean of natural runoff; $\overline{Q_{sim}}$ = mean of simulated runoff; n = simulating length.

Downscaling global circulation model outputs

GCMs are generally not appropriate for finer-scale impact modelling because of their low spatial resolution and the greater uncertainty in their outputs at fine temporal resolution. To date, the delta method is the most commonly used method of transmission. Due to the characteristics of simple operation, which inserts the anomalies of GCM cell centroids and is applied to a baseline climate given by a high-resolution surface, the delta method has been the most popular approach (Ivanov & Kotlarski 2017). Compared with some other downscaling methods, this approach makes it easy to estimate the difference between the present and future climate without numerous simulations of the relationship among multiple meteorological elements (Ramirez-Villegas & Jarvis 2010; Eum & Cannon 2017; Keller *et al.* 2017).

In this method, two time series (1966–2005 and 2011–2050) of the predictor variables were extracted from the three GCMs for the grid box. In this paper, the delta change method is used to downscale precipitation (P), and maximum and minimum temperature ($T_{\max}$ and $T_{\min}$):

$$P_{future}(x, t) = P_{station}(x, t)^* \frac{[P_{Gfuture}]_{mon}}{[P_{Ghistory}]_{mon}} \quad (4)$$

$$T_{future}(x, t) = T_{station}(x, t) + \left\{ [T_{Gfuture}]_{mon} - [T_{Ghistory}]_{mon} \right\} \quad (5)$$

where $P_{future}(x, t)$ and $T_{future}(x, t)$ are the downscaled P and T for the grid containing a location x and at time t, $P_{station}(x, t)$ and $T_{station}(x, t)$ represent the simulated monthly mean precipitation for the grid containing a location x and at time t, $[P_{Ghistory}]_{mon}$, $[P_{Gfuture}]_{mon}$, $[T_{Ghistory}]_{mon}$ and $[T_{Gfuture}]_{mon}$ are the monthly data means from the grid, taken over the fitting period from the GCMs.

Control variable method and simulation schemes settings

The use of the control variables method in this paper is intended to address the following requirements: (1) To judge whether the effect on a variable by an independent variable is direct and determine if the independent variable has a causal effect on the dependent variable; (2) to judge the degree of those effects if several independent variables all have causal effects on the dependent variable; and (3) to judge whether the relationship between variables changes under differing conditions (Smelser & Baltes 2001; Pedhazur & Schmelkin 2013). In this paper, the independent variables were P, $T_{\min}$ and $T_{\max}$, and the dependent variable was R. We used the control variable method to create a set of contrasting simulations according to the possible combinations of un-scaled or scaled meteorological elements, which would be available for a follow-up study.

Table 1 | Set of meteorological elements change schemes

Simulation scheme	Meteorological elements scaling	
	Scaling	**No scaling**
I	None	Both the maximum temperature, the minimum temperature and precipitation
II	Precipitation	The maximum temperature, the minimum temperature
III	The maximum temperature	Precipitation, the minimum temperature
IV	The minimum temperature	Precipitation, the maximum temperature
V	Precipitation, the minimum temperature	The maximum temperature
VI	Precipitation, the maximum temperature	The minimum temperature
VII	The minimum temperature, the maximum temperature	Precipitation
VIII	Both the maximum temperature, the minimum temperature and precipitation	None

Table 1 lists a set of simulations according to eight possible combinations of unscaled or scaled precipitation and the maximum and minimum temperature data (Bosshard *et al.* 2014). By assessing the amount of runoff change under different schemes, we determined the most sensitive element and season that influence the runoff, and we then quantitatively evaluated their level of sensitivity.

Qualitatively, the greater the deviation in the separate effect schemes (using either the $T_{\min}$, $T_{\max}$ or P effect: scheme IV, III, II, respectively) following the initial simulation (scheme I), the greater the influence of meteorological elements on the runoff. In other words, the runoff is more sensitive to the meteorological elements. The closer the scheme results follow the full simulation (scheme VIII), the higher the contribution of the meteorological elements of the scheme. In contrast, the lack of meteorological elements in a scheme produces a lesser effect on the runoff.

The sensitivity of runoff to precipitation and temperature changes under the different climate-change scenarios can be expressed as the changes in runoff simulation for each scheme in a 40-yr time series by using the VIC model, which can be estimated as:

$$\varepsilon_i = \frac{\Delta R_i}{R_{\mathrm{I}}} \times 100\% = \frac{R_{\mathrm{I}} - R_i}{R_{\mathrm{I}}} \times 100\% \tag{6}$$

where ε_i represents the sensitivity coefficients of runoff to scheme $i (i = \mathrm{II}, \mathrm{III}, \cdots, \mathrm{VIII})$ scaled meteorological elements under the different climate-change scenarios. ΔR_i denotes the runoff changes due to the scheme i influencing factor. R_{I} and R_i denotes the simulation of runoff under scheme I and scheme i, respectively.

RESULTS AND DISCUSSION

Calibration and validation

Figure 2 presents the validation of the simulated mean annual runoff, which indicates a good simulated effect for the calibration period of 1966–1975 and validation period of 1976–1985. The runoff has a peak, with mean runoff occurring in summer (from June to August) at Maqu and Tangnaihai. The model slightly overestimates the mean runoff in spring (from March to May) and summer. In autumn (from September to November) and winter (from December to February of the following year), the model shows a systematic negative bias. Table 2 presents the values of the VIC model performance over the calibration period and validation period. The validation period using the Nash–Sutcliffe efficiency shows increasing performance when moving downstream. The value of E_r between the simulated values and the observed values was −2.41% at the Maqu station and −6.37% at the Tangnaihai station during the calibration period. Compared with the results of the calibration period, the values of E_r are smaller during the validation period. The N_s value of the

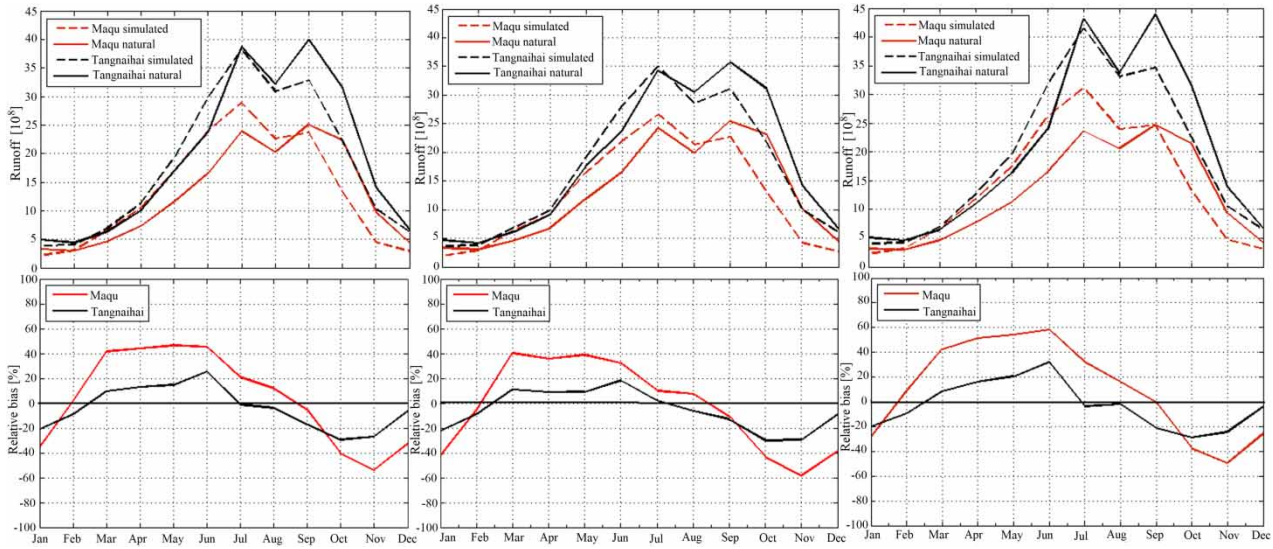

Figure 2 | (Top) Natural and simulated average monthly runoff within the SRYR. (Bottom) Relative bias of simulated vs natural monthly runoff. (Left) The entire control period, (Middle) the calibration period, and (Right) the validation period.

calibration period is usually higher than the validation period. N_s is greater than 0.7 for the Maqu and Tangnaihai stations, although it is relatively low (0.66) for the Maqu station during the validation period. This result indicates that VIC can simulate natural runoff relatively well in the two watersheds. The values of R from the two stations are greater than 0.8. The higher the correlation coefficient, the greater the correlation between the simulation and natural runoff.

Climate-change projections

Due to simplification of climate representation, potentially wrong assumptions about climate processes, limited spatial and temporal resolution, and errors in the forcing data, the predictions of meteorological elements by GCMs are known to contain large uncertainty and further cause hydrological simulation deviations (Maurer 2007; Nobrega *et al.* 2011; Shen *et al.* 2018). Thus, the use of a multi-model ensemble is recommended when implementing climate change studies. Based on the different prediction results of meteorological factors, the impacts of climate change on runoff under the different climate scenarios are researched in terms of changing the input of the distributed hydrological model to simulate runoff because of the uncertainty of factors such as GCMs and climate scenarios.

Table 2 | Evaluation of simulation results for model performance of monthly runoff in the SRYR

	Calibration period (1966–1975)			Validation period(1976–1985)		
Station	N_s	E_r/%	R	N_s	E_r/%	R
Maqu	0.71	−2.41	0.85	0.66	–0.13	0.82
Tangnaihai	0.88	−6.37	0.94	0.80	–4.78	0.90

Climate model regional applicability

The verification results show that three GCMs can pretty well simulate the large-scale characteristics of temperature (see Figure 3). In addition, the values of the coefficient of determination (R^2) for the monthly minimum temperature and maximum temperature are greater than 0.9. Although the simulation of precipitation has a large positive error, the values of the coefficient of determination (R^2) are almost 0.7 for precipitation. These values show that the selected climate models applicable to this region have relatively good agreement with the observed meteorological data and GCMs output data.

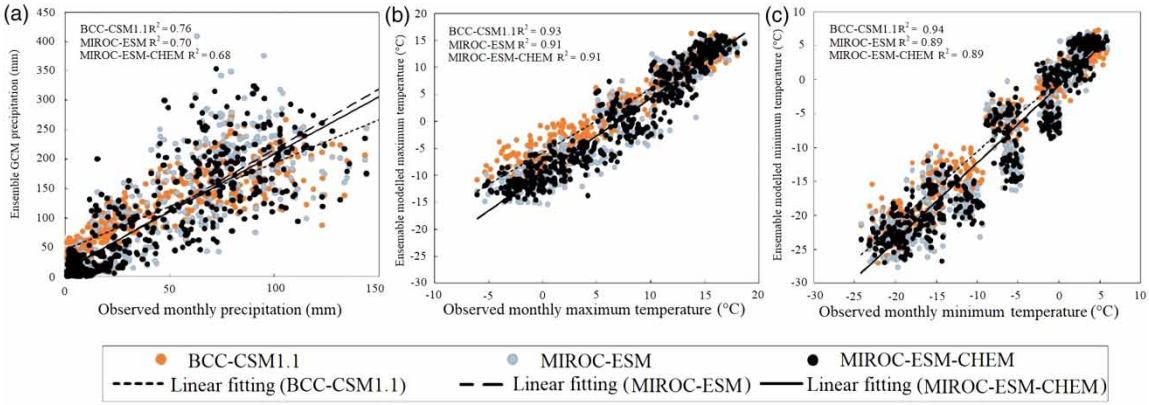

Figure 3 | Scatter plots for observed meteorological data and GCMs output data from 1966–2005: (a) precipitation, (b) minimum temperature and (c) maximum temperature.

Spatial distribution characteristics

Figure 4 shows the spatial distribution of precipitation, maximum temperature, minimum temperature and runoff during the historical period (1966–2005). The hydrological conditions of the various geographical locations are very different, considering the impact of the East Asian monsoon and the elevation (Hu *et al.* 2012). The temperature and precipitation decrease gradually from southeast to northwest. The summer monsoon brings plentiful precipitation to the study region, and while drought frequently occurs during the winter, the region is characterized by hot, rainy summers and cold, dry winters (Yang *et al.* 2007). The southeastern part of this region has the most precipitation, and the precipitation in summer was greater than 350 mm. Precipitation critically influences the spatial distribution of hydrological fluxes, especially in runoff. In summer

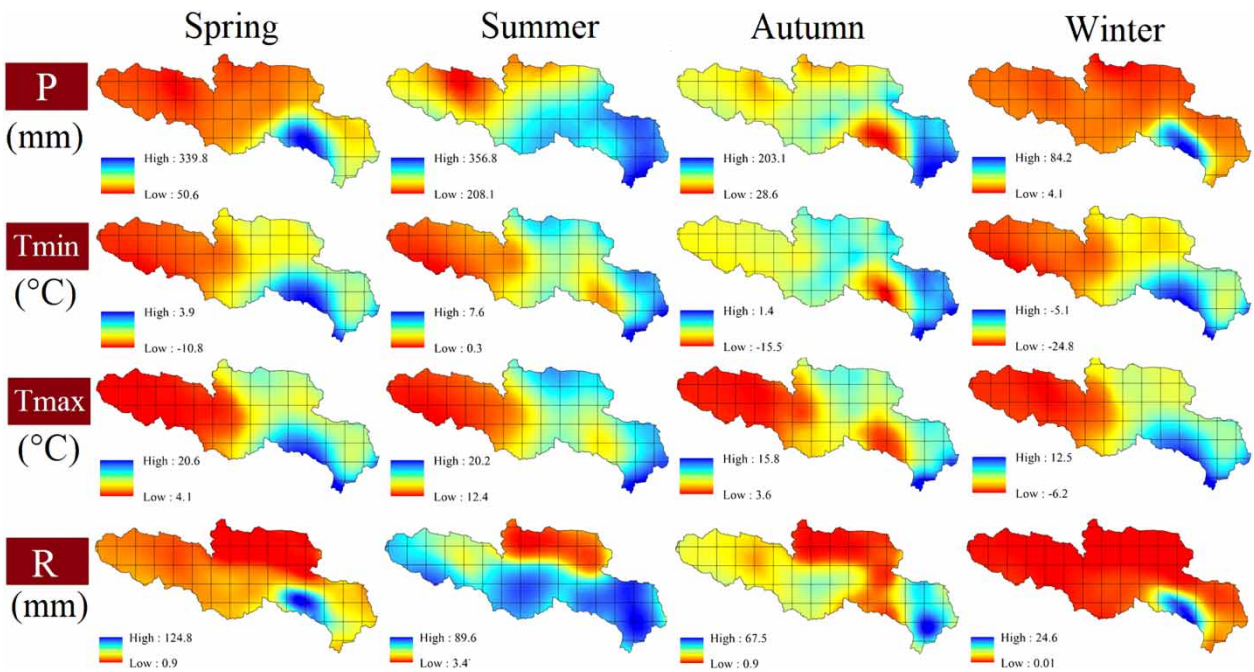

Figure 4 | The spatial distribution meteorological elements in the historical period (1966–2005).

and winter, the spatial variability of the runoff yield is more obvious than that of precipitation.

Precipitation changes

Our results demonstrate that the evaluated climate change projections of precipitation clearly differ from the GCMs or scenarios. Even where the models agree on the direction of precipitation change, there are considerable differences in magnitude. Compared to two other GCMs, on the basis of the absolute value of regional precipitation changes in the peak and valley of each season, the BCC-CSM1.1 model has the smallest peak-valley difference and therefore has less regional differences. In addition, the difference between present and future precipitation projected by BCC-CSM1.1 was significantly smaller than that projected in absolute numbers by MIROC-ESM and MIROC-ESM-CHEM. The ensemble mean changes (the average of all GCMs) in average annual precipitation are +8.7% for RCP4.5 and +9.7% for RCP8.5 at the control area of the Maqu station and +7.0% for RCP4.5 and +7.7% for RCP8.5 at the control area of the Tangnaihai station. In this significantly water-scarce basin, projected increasing precipitation may help to both mitigate the harm caused by continuous droughts and have a positive effect on the social ecosystem.

Our results also indicate that climate change projections of precipitation vary distinctly with region and season (see Figure 5). Compared with other seasons, in winter, precipitation increases significantly, with an increase greater than 50% in some areas under the MIROC-ESM and MIROC-ESM-CHEM models. In the projections of precipitation changes for spring and winter, all models except for BCC-CSM1.1 project

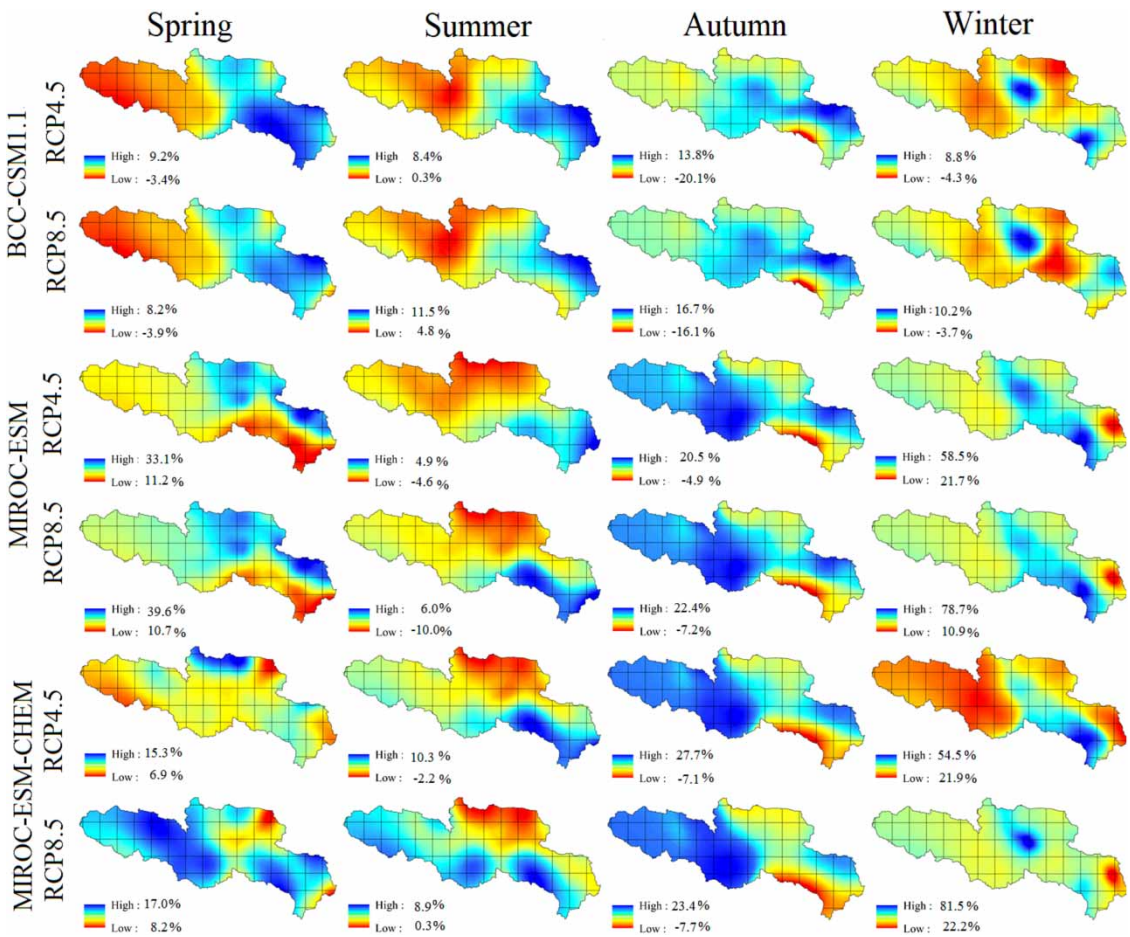

Figure 5 | The relative change (%) in predicted average precipitation from the historical data for different scenarios.

a significant increase in P for the whole study region. In summer, precipitation increases in the study area in BCC-CSM1.1, but the other two models have a negative P change signal from the northern region. For autumn, all model results show an increase in P for almost the whole study region, apart from some areas that have so much rainfall that they probably appear in the negative P change signal from the southern region.

Maximum and minimum temperatures changes

Temperature has a much higher degree of consistency in its spatial pattern trends than precipitation. All GCM model results show a temperature increase in all seasons throughout the year, but there were obvious changes in the magnitude of the variation in different seasons using the same GCM and using different GCMs for the same season. Moreover, for all models, the temperature increase in the RCP8.5 scenario is greater than that in the RCP4.5 scenario. For example, in the case of the control area in the Tangnaihai station, the magnitudes of increases in minimum temperature are approximately 1.60 and 1.98 °C (RCP4.5 and RCP8.5, respectively), whereas for the maximum temperature, the increases in temperature are approximately 1.36 and 1.69 °C, respectively. This result is consistent with the ranking of the changes for the representative concentration path scenarios setting.

Analysis of the spatial distribution of the maximum and minimum temperature produced a variety of trends (see Figure 6). The maximum and minimum spatial distribution variations in temperature in the study region are clearly different under different GCM scenarios and sometimes even totally opposite in the northwest part, during winter. In the projections of seasonal temperature changes, all models agree on the phenomenon that the increase in the minimum temperature is greater than that of the maximum temperature. The increase in the magnitude of the maximum and minimum temperatures is larger in spring and autumn, and the increase in the magnitude of the temperature in the upstream station (Maqu) was significantly higher than that of the downstream station (Tangnaihai).

Impact of climate change on runoff

All of the GCMs except for BCC-CSM1.1 are consistent in projecting an increase in runoff, and the spatial and temporal variability of runoff is more complex than that for precipitation. The BCC-CSM1.1 model is obviously distinct from the other two GCMs, having both smaller amplitude of variation and a complex spatial variation (see Figure 7). The BCC-CSM1.1 model also projects a decrease in runoff, and the results are consistent with the significantly lesser increase in precipitation and larger range of temperature rise, especially in spring. With the change in meteorological elements at the outlet station Tangnaihai and for the period 2011–2050, the magnitude of projected annual runoff changes varies between −0.4 and 9.5% under the RCP4.5 scenarios, depending on the climate scenario used, while the magnitude varies between 0.6 and 9.3% under the RCP8.5 scenarios.

The runoff at the Tangnaihai station shows smaller increases than the runoff at the Maqu station in certain scenarios, despite the potentially higher increases in precipitation. Seasonally, spring and winter runoff showed dramatic increases under the MIROC-ESM and MIROC-ESM-CHEM models. The average change rates are +22.2% for spring and +15.5% for winter, especially west of the study area, where the elevation was higher. This result may be related to increasing temperatures, with more of the winter precipitation falling as rain and effectively becoming runoff instead of being stored in the snowpack until the melt season.

The relative changes in seasonally climatic variables were studied from spring to winter (Figure 8). Generally, almost all model temperature variation points are below the diagonal, which means the increase in the minimum temperature is higher than that of the maximum temperature. This result is consistent with the previous discussion. For precipitation and runoff, the rate of change in precipitation is higher than the rate of change in runoff in autumn and winter, as the situation is more complicated in spring and summer. The range of variability for precipitation and runoff in spring is much broader than in other seasons and is more concentrated in summer and autumn.

Runoff sensitivity to precipitation and temperature changes

Simulation schemes results

This section assesses the sensitivity of runoff to precipitation and temperature changes under the different climate change scenarios and identifies the separate and interacting effects of changes in meteorological elements of runoff. Simulation

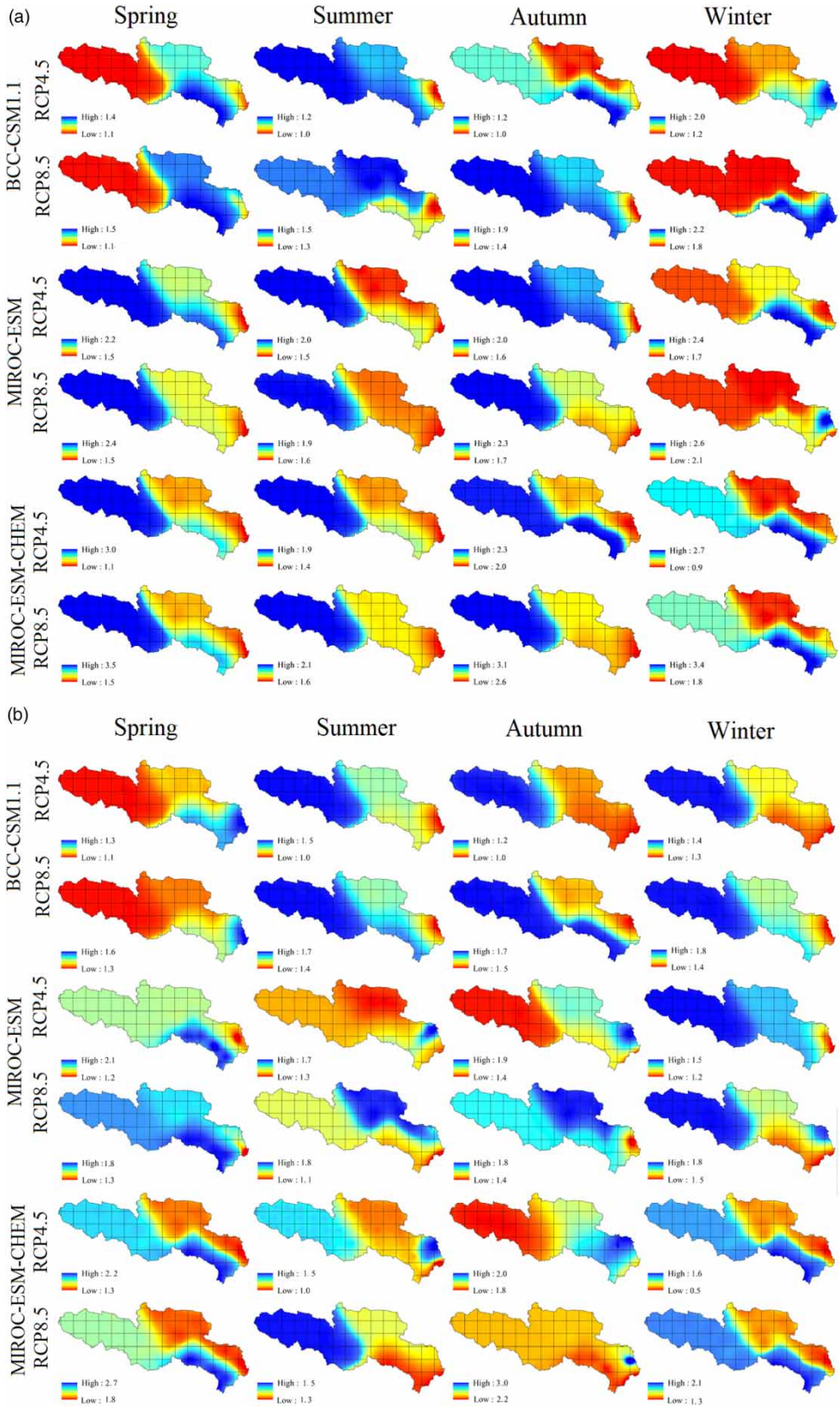

Figure 6 | The spatial variations of predicted temperature (°C) from the historical data for different scenarios. (a) the T_{min} results of scenarios; (b) the T_{max} results of scenarios.

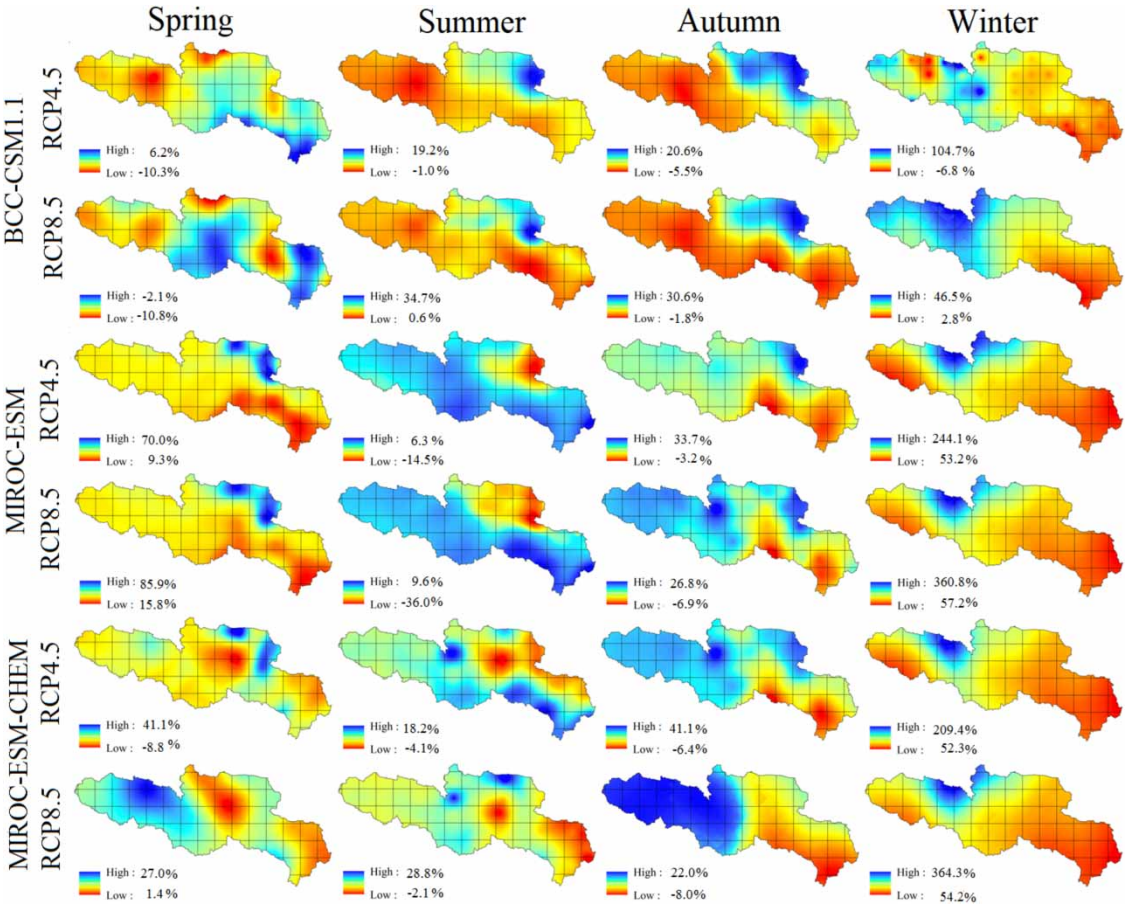

Figure 7 | The spatial variations in predicted runoff from the historical data for different scenarios.

results are shown for each scheme in a 40-yr time series of simulated daily runoff using the VIC model (Table 3).

To ensure that the assessment is hierarchical and comparable, the scheme established in this article proposes to classify the assessment into separate element effects and to combine these element effects according to their different purposes. Figure 9 shows the differences in the annual cycles of runoff between the periods 2011–2050 and 1966–2005, as projected by the separate meteorological element effect schemes, as well as by the full simulation of all three of the T_{min}, T_{max} and P effects at selected stations.

The separate effects of changes in meteorological elements on runoff

Generally, from the comparison of the results for schemes II, III, and IV (Figure 10) in the study region (for both the Maqu station and the Tangnaihai station), we found that there is an obvious difference in the impacts that the meteorological elements have on the runoff. Precipitation changes determine the changes in seasonal runoff to a large degree (consistent with Jones *et al.* (2006) and Zhang *et al.* (2017) studies), with a 23% degree of influence relative to baseline period runoff, followed by the effects of maximum temperatures (approaching 12%) and minimum temperatures (approaching 3%). The T_{max} effect outclasses the T_{min} effect, despite the fact that the increase in the T_{min} magnitude is probably greater than that of T_{max}.

Taking the effect of P as an example, the seasonal differences in the climate scenarios are analysed. In spring, the P effect of MIROC-ESM has the maximum amplification rate; In contrast, in summer and winter, it is the P effect of MIROC-ESM-CHEM. For autumn, the differences among the amplitudes of the P effect in all scenarios are slight. In the

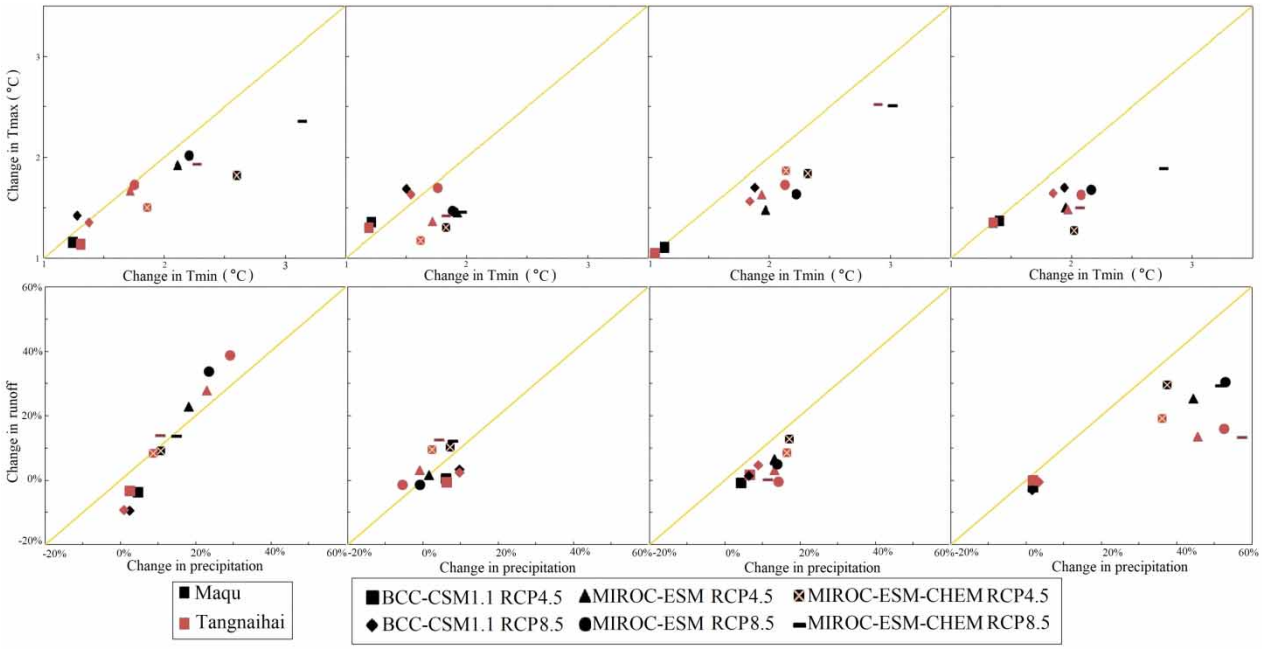

Figure 8 | Relative changes in seasonal precipitation, maximum and minimum temperature, and runoff.

Table 3 | Comparison of the mean annual runoff for the T_{max}, T_{min} and P effect schemes program with the initial program (scheme I)

			Simulation scheme (%)						
Station	**GCM**	**Scenario**	**II**	**III**	**IV**	**V**	**VI**	**VII**	**VIII**
Maqu	BCC-CSM1.1	RCP4.5	13.4	−9.7	−2.9	10.4	3.2	−12.9	−0.8
		RCP8.5	17.6	−12.3	−2.9	14.6	4.2	−15.9	−0.3
	MIROC-ESM	RCP4.5	24.7	−10.6	−4.1	19.5	12.3	−15.7	8.7
		RCP8.5	26.4	−11.1	−4.1	20.8	13.3	−16.2	9.6
	MIROC-ESM-CHEM	RCP4.5	28.9	−10.7	−4.2	23.5	15.9	−16.1	11.5
		RCP8.5	31.1	−12.5	−4.3	25.2	15.7	−18.4	11.6
Tangnaihai	BCC-CSM1.1	RCP4.5	14.6	−10.8	−2.3	12.2	3.1	−13.5	−0.4
		RCP8.5	19.5	−13.7	−2.0	17.4	4.5	−16.7	0.6
	MIROC-ESM	RCP4.5	25.1	−12.0	−3.3	20.8	11.4	−16.4	8.3
		RCP8.5	25.5	−13.1	−3.2	20.9	10.7	−17.6	7.3
	MIROC-ESM-CHEM	RCP4.5	27.6	−12.1	−3.4	23.3	13.5	−16.8	9.5
		RCP8.5	29.4	−14.3	−3.3	24.8	12.6	−19.5	9.3

BCC-CSM1.1 model, the P effect determines the runoff change more significantly from July to September. In the remaining two models, MIROC-ESM and MIROC-ESM-CHEM, the P effect is more significant in determining the runoff change from April to June and from May to July, respectively.

The scheme results further show that the impacts of the changes in meteorological elements on runoff in different seasons and at different stations vary. For simplicity, a brief analysis of the BCC-CSM1.1 RCP4.5 scenario is provided with the expectation that similar results can be obtained when using the other model.

Comparing the results of the two stations from the perspective of annual change, the meteorological element effects at the Tangnaihai station are all greater than those at the Maqu station. From the perspective of seasonal change, the meteorological effects in spring are consistent with annual changes. However, in summer and autumn, the meteorological effects at the Tangnaihai station are greater than those at the Maqu

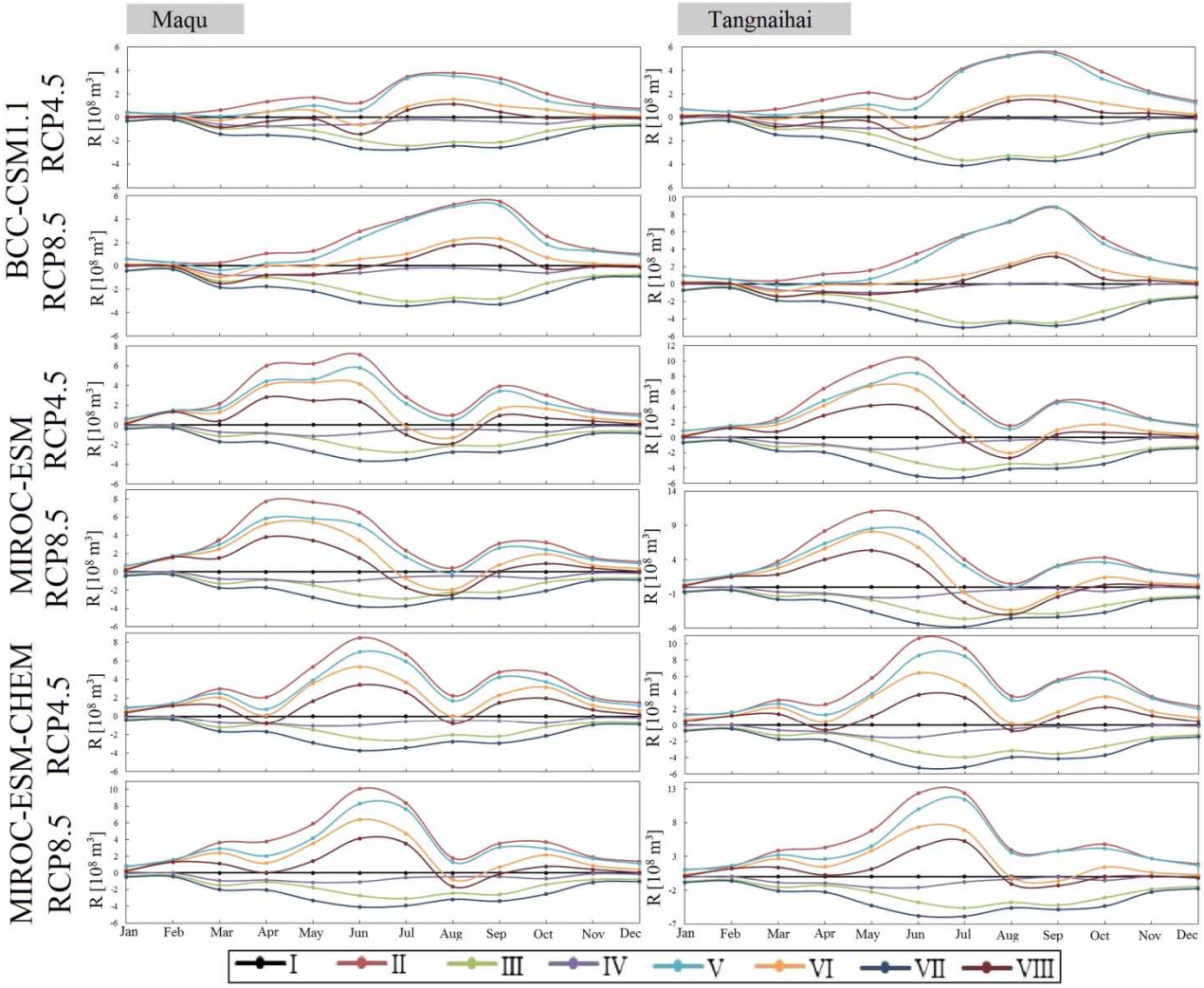

Figure 9 | The differences between the future period (2011–2050) and the historical period (1966–2005) in the annual cycle of runoff (R) at the stations resulting from the change schemes of meteorological elements.

station for both the P and T_{max} effect but smaller for the T_{min} effect. In winter, the meteorological effects at the Tangnaihai station are all smaller than those at the Maqu station. A comparison of the four seasons shows that winter is the season during which runoff is most sensitive to precipitation and maximum temperature changes; in terms of the minimum temperature, runoff is the most sensitive in spring.

The interacting effects of changes in meteorological elements on runoff

When the separate effects of P, T_{max} and T_{min} are added together, this sum more closely follows the full simulation, and the effects of the meteorological elements are more linear. Thus, a given magnitude change in any one of the elements has the same effect on runoff. The results show that although the meteorological elements effects are close to being additive, at least in principle, there are still gaps. This scenario means that the external environment will affect runoff sensitivities to precipitation and temperature changes. Therefore, this section addresses the need to analyse the interacting effects of changes in meteorological elements on runoff, understanding the influence of external climatic conditions on the degree of runoff sensitivities to precipitation and temperature changes, and quantification of the variation ranges.

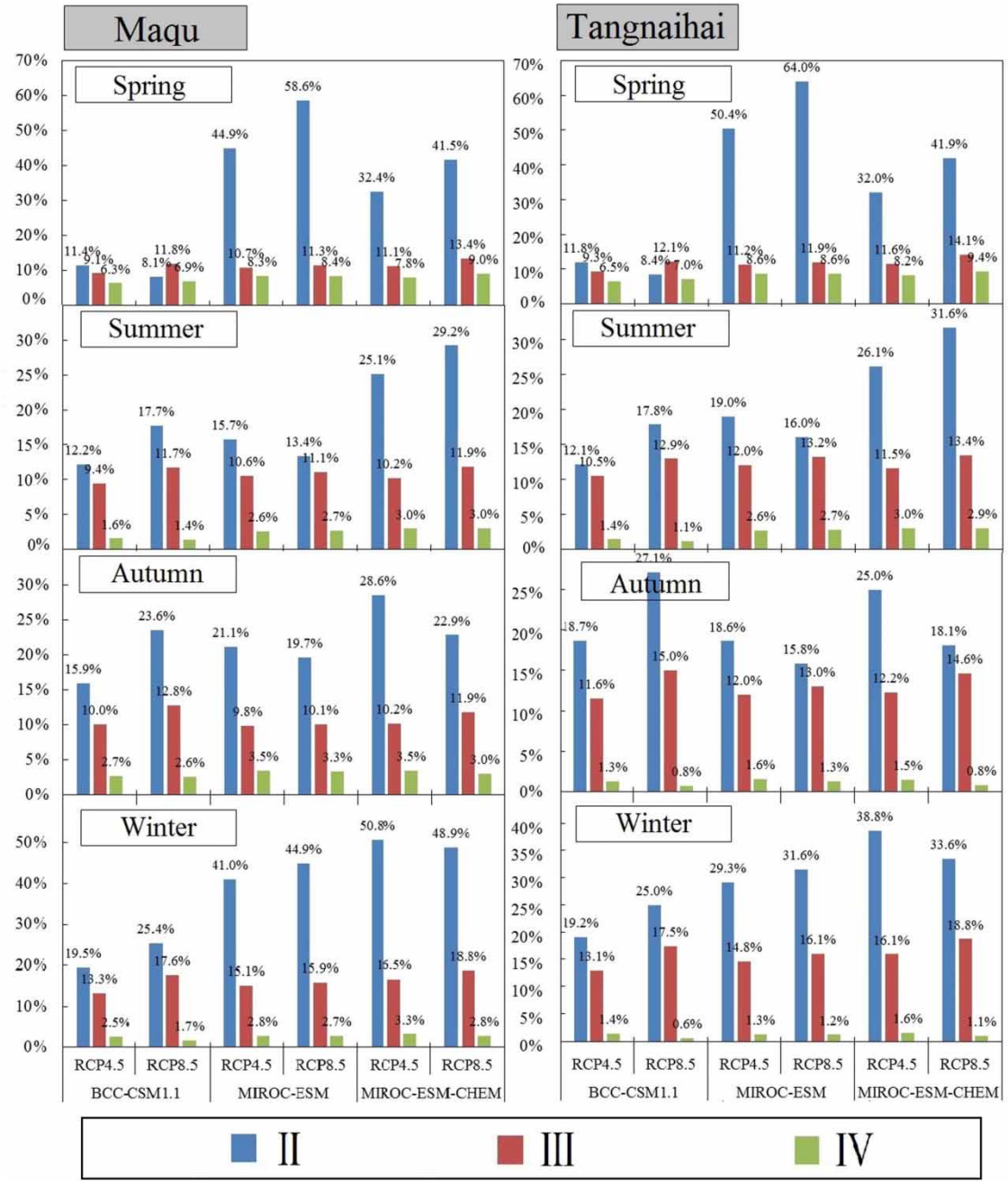

Figure 10 | Contributions of the effects of meteorological element changes to changes in the seasonal runoff at two stations in the study region.

As an example of this type of analysis, Figure 11 is the result of the BCC-CSM1.1 RCP4.5 scenarios. An analysis of the P effect under different external environmental conditions shows that: (1) with the T_{min} changes, all seasons except summer exhibit a slight decrease in the P effect in comparison with the historical condition; (2) with the T_{max} changes, all seasons except spring exhibit a significantly decreased P effect, and the range of the decrease for the Maqu station is far higher than that for the Tangnaihai station; (3) with the T_{max} and T_{min} changes, it can be seen that all seasons have decreased to the lowest P effect; and (4) the gap in the P effect between the stations differs

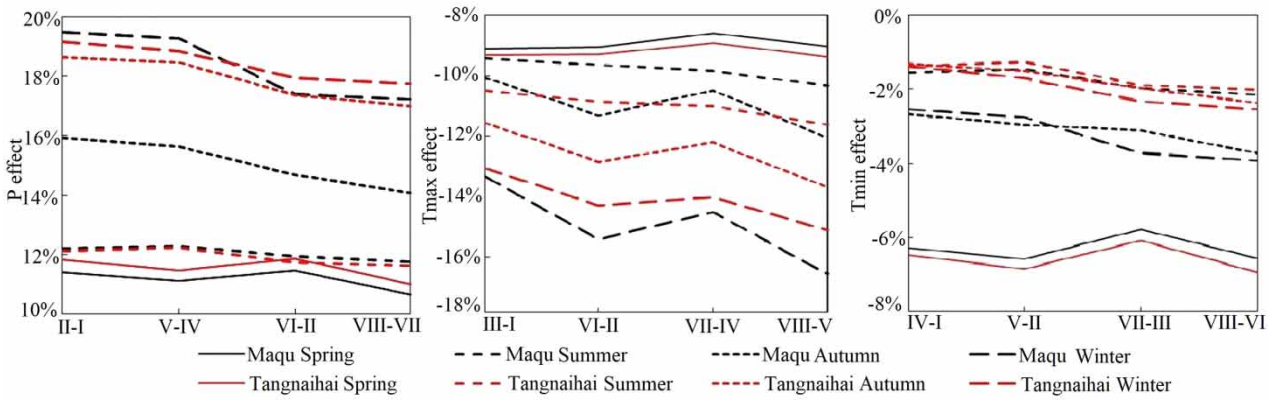

Figure 11 | The influence of external climatic conditions on the levels of runoff sensitivities to precipitation and temperature changes. The style of the abscissa is 'A-B'. The abscissa measures how much of the projected changes are explained by a single effect (T_{max}, T_{min} or P) when converted to the 'A' situation in the context of the 'B' situation.

significantly and shows volatile fluctuation in autumn, and there is the smallest gap in the summer season. Compared with the other seasons, in the spring, the P effect is very different and even appears to grow under the condition of T_{max}.

The results of the analysis of the T_{max} effect under different external environment conditions show that: (1) compared with the P and T_{min} effects, the T_{max} effect of the regional external environment fluctuated greatly; (2) under the condition of P changes, all seasons except spring exhibit a significant decrease in the T_{max} effect in comparison with the historical environment; and (3) under the condition of T_{min} changes, spring exhibits a significant increase in the T_{max} effect. The other seasons show a slight decrease compared with the historical environment; (4) under the condition of P and T_{min} changes, it can be seen that all seasons except spring show the lowest T_{max} effect. Even for spring, the magnitude of growth decreases compared to the condition of T_{min}. However, the T_{max} effect shows a small increase under the condition of changes in P.

The results of analysing the T_{min} effect under different external environment conditions show that: (1) under the condition of P changes, all seasons exhibit a slight decrease in the T_{min} effect compared with the historical environment; (2) under the condition of T_{max} changes, all seasons except spring agree on a significant decrease in the T_{min} effect compared with the historical environment, with spring showing a significant increase; (3) under the condition of P and T_{max} changes, it can be seen that all seasons except spring show the lowest T_{min} effect. Even for spring, the magnitude of growth decreases, compared to the condition of T_{max} changes. In other words, T_{max} and T_{min} weaken the power of each other in spring, under the condition of P changes.

CONCLUSIONS

In this paper, we investigate the hydrological response to future climate change in a case study of the SRYR, where the water resources system is very sensitive to climate change, using the VIC model with the delta change method with different CMIP5 RCP scenarios. Based on the changing characteristics of hydrological elements, as well as meteorological elements including precipitation (P), the minimum and maximum temperature (T_{min} and T_{max}) are obtained from nine modelling schemes with the control variable method that uses the same parameters of the model over the baseline period (1966–2005) with CMIP5 RCP scenarios in RCP4.5 and RCP8.5. The contribution of changes in meteorological factors to runoff at seasonal scales are then quantified. Through the assessment of the amount of runoff change under different schemes, we determined the most sensitive element and season that influences the runoff, and we then quantitatively evaluated their levels of sensitivity. Furthermore, to better understand the influence of external climatic conditions on the levels of runoff sensitivities to precipitation and temperature changes, we also conducted a comparative study on the

amount of runoff change under combined meteorological element schemes.

The results show that the projected precipitation suggests a general increase, with a larger level either in summer or winter depending on the GCMs used. All scenarios show clearly warming trends in each season, with a larger level in winter, noting particularly that the minimum temperature warming rate is higher than that of the maximum temperature. According to the results of statistical analysis, the magnitude of runoff changes depends considerably on the GCMs (Xu *et al.* 2009). These results are in good agreement with those by Zhang *et al.* (2017), and they also provide a detailed analysis of the seasonal scale. A large increase in precipitation and rapidly warming temperature are the prominent reasons for the runoff changes (Tang *et al.* 2012). We found that there is an obvious difference in the impact that the meteorological elements have on the runoff. The effect of precipitation changes determines the changes in seasonal runoff to a large degree (consistent with previous studies), with a 23% degree of influence relative to baseline period runoff, followed by the effects of maximum temperatures (approaching 12%) and the minimum temperatures (approaching 3%). The effect of maximum temperature changes is outclassed by that of the minimum temperature changes (Liu *et al.* 2017), despite the fact that the magnitude of increase in the minimum temperature is greater than that of the maximum temperature. Winter is the season that displays the greatest sensitivity of runoff to precipitation and maximum temperature change; but for the minimum temperature change, spring is the most sensitive season. The levels of runoff sensitivities to precipitation and temperature changes vary with different external climatic conditions. The gap in the P effect between the stations differs significantly and shows volatile fluctuation in autumn, with the smallest gap occurring in the summer season. T_{max} and T_{min} weaken the power of each other in spring under the condition of P changes.

Great efforts have been made to fully assess runoff sensitivities to precipitation and temperature changes in this study; however, further research is required on the impact of frozen ground degradation on runoff and other indirect effects caused by temperature increases (Li *et al.* 2017a; Wang *et al.* 2018). A series of limitations exists in the process of hydrological modelling simulations (Mockler *et al.* 2016; Trudel *et al.* 2017), although previous studies have shown that GCMs are the most important factor of uncertainty in hydrological simulation. However, other uncertainty factors such as downscaling methods and types of hydrological models have also been found to have great significance in hydrological simulations (Teutschbein *et al.* 2011; Srivastava *et al.* 2014; Yuan *et al.* 2017). Although three GCMs and two emission scenarios were used in this study, other uncertainties were not taken into account. Therefore, a comprehensive analysis of the uncertainty effects in hydrological simulation will be emphasized in further research.

ACKNOWLEDGEMENTS

This research was supported by the National Key Research and Development Program of China (2017YFC0404404), the National Science Foundation of China (91647112, 51679187), and Doctor Innovation Foundation of Xi'an University of Technology (310-252071605). Sincere gratitude is extended to the editor and the anonymous reviewers for their professional comments and suggestions.

REFERENCES

Andrews, T., Gregory, J. M. & Webb, M. J. 2015 The dependence of radiative forcing and feedback on evolving patterns of surface temperature change in climate models. *J. Clim.* **28** (4), 1630–1648.

Bates, B. C., Kundzewicz, Z. W., Wu, S. & Palutikof, J. P. (eds). 2008 *Climate Change and Water*. IPCC Technical paper. Intergovernmental Panel on Climage Change, Geneva.

Bhatti, A. M., Koike, T. & Shrestha, M. 2016 Climate change impact assessment on mountain snow hydrology by water and energy budget-based distributed hydrological model. *J. Hydrol.* **543**, 523–541.

Bosshard, T., Kotlarski, S., Zappa, M. & Schär, C. 2014 Hydrological climate-impact projections for the Rhine River: GCM–RCM uncertainty and separate temperature and precipitation effects. *J. Hydrometeorol.* **15** (2), 697–713.

Bowling, L. C. & Lettenmaier, D. P. 2010 Modeling the effects of lakes and wetlands on the water balance of Arctic environments. *J. Hydrometeorol.* **11** (2), 276–295.

Brikowski, T. H. 2015 Applying multi-parameter runoff elasticity to assess water availability in a changing climate: an example from Texas, USA. *Hydrol. Process.* **29** (7), 1746–1756.

Chang, H. & Jung, I. W. 2010 Spatial and temporal changes in runoff caused by climate change in a complex large river basin in Oregon. *J. Hydrol.* **388** (3), 186–207.

Dibike, Y. B. & Coulibaly, P. 2005 Hydrologic impact of climate change in the Saguenay watershed: comparison of downscaling methods and hydrologic models. *J. Hydrol.* **307** (1–4), 145–163.

Dosio, A. & Panitz, H. J. 2016 Climate change projections for CORDEX-Africa with COSMO-CLM regional climate model and differences with the driving global climate models. *Clim. Dyn.* **46** (5–6), 1599–1625.

Drogue, G., Pfister, L., Leviandier, T., El Idrissi, A., Iffly, J. F., Matgen, P., Humbert, J. & Hoffmann, L. 2004 Simulating the spatio-temporal variability of streamflow response to climate change scenarios in a mesoscale basin. *J. Hydrol.* **293** (1), 255–269.

Eum, H. I. & Cannon, A. J. 2017 Intercomparison of projected changes in climate extremes for South Korea: application of trend preserving statistical downscaling methods to the CMIP5 ensemble. *Int. J. Climatol.* **37** (8), 3381–3397.

Fan, H., Xu, L., Tao, H., Feng, W., Cheng, J. & You, H. 2017 Accessing the difference in the climate elasticity of runoff across the Poyang Lake Basin, China. *Water* **9** (2), 135.

Gao, Z., Zhang, L., Zhang, X., Cheng, L., Potter, N., Cowan, T. & Cai, W. Z. 2016 Long-term streamflow trends in the middle reaches of the Yellow River Basin: detecting drivers of change. *Hydrol. Process.* **30** (9), 1315–1329.

Gosling, S. N. & Arnell, N. W. 2016 A global assessment of the impact of climate change on water scarcity. *Clim. Change* **134** (3), 371–385.

Gregoretti, C., Degetto, M., Bernard, M., Crucil, G., Pimazzoni, A., De Vido, G., Berti, M., Simonl, A. & Lanzoni, S. 2016 Runoff of small rocky headwater catchments: field observations and hydrological modeling. *Water Resour. Res.* **52** (10), 8138–8158.

Hu, Y., Maskey, S. & Uhlenbrook, S. 2012 Trends in temperature and rainfall extremes in the Yellow River source region, China. *Clim. Change* **110** (1–2), 403–429.

Huang, S., Huang, Q., Leng, G., Zhao, M. & Meng, E. 2017 Variations in annual water-energy balance and their correlations with vegetation and soil moisture dynamics: a case study in the Wei River Basin, China. *J. Hydrol.* **546**, 515–525.

Huziy, O. & Sushama, L. 2017 Impact of lake–river connectivity and interflow on the Canadian RCM simulated regional climate and hydrology for Northeast Canada. *Clim. Dyn.* **48** (3–4), 709–725.

Immerzeel, W. W., Van Beek, L. P. & Bierkens, M. F. 2010 Climate change will affect the Asian water towers. *Science* **328** (5984), 1382–1385.

Ivanov, M. A. & Kotlarski, S. 2017 Assessing distribution-based climate model bias correction methods over an alpine domain: added value and limitations. *Int. J. Climatol.* **37** (5), 2633–2653.

Jones, R. N., Chiew, F. H., Boughton, W. C. & Zhang, L. 2006 Estimating the sensitivity of mean annual runoff to climate change using selected hydrological models. *Adv. Water Resour.* **29** (10), 1419–1429.

Keller, D. E., Fischer, A. M., Liniger, M. A., Appenzeller, C. & Knutti, R. 2017 Testing a weather generator for downscaling climate change projections over Switzerland. *Int. J. Climatol.* **37** (2), 928–942.

Li, H., Zhang, Q., Singh, V. P., Shi, P. & Sun, P. 2017a Hydrological effects of cropland and climatic changes in arid and semi-arid river basins: a case study from the Yellow River basin, China. *J. Hydrol.* **549**, 547–557.

Li, J., Shi, J., Zhang, D. D., Yang, B., Fang, K. & Yue, P. H. 2017b Moisture increase in response to high-altitude warming evidenced by tree-rings on the southeastern Tibetan Plateau. *Clim. Dyn.* **48** (1–2), 649–660.

Liang, X., Lettenmaier, D. P., Wood, E. F. & Burges, S. J. 1994 A simple hydrologically based model of land surface water and energy fluxes for general circulation models. *J. Geophys. Res. Atmos.* **99** (D7), 14415–14428.

Liu, Z., Xu, Z., Fu, G. & Yao, Z. 2013 Assessing the hydrological impacts of climate change in the headwater catchment of the Tarim River basin, China. *Hydrol. Res.* **44** (5), 834–849.

Liu, J., Zhang, Q., Singh, V. P. & Shi, P. 2017 Contribution of multiple climatic variables and human activities to streamflow changes across China. *J. Hydrol.* **545**, 145–162.

Ma, M., Ren, L., Singh, V. P., Yuan, F., Chen, L., Yang, W. & Liu, Y. 2016 Hydrologic model-based Palmer indices for drought characterization in the Yellow River basin, China. *Stoch. Environ. Res. Risk Assess.* **30** (5), 1401–1420.

Maurer, E. P. 2007 Uncertainty in hydrologic impacts of climate change in the Sierra Nevada, California, under two emissions scenarios. *Clim. Change* **82** (3–4), 309–325.

Mishra, V., Cherkauer, K. A. & Bowling, L. C. 2011 Changing thermal dynamics of lakes in the Great Lakes region: role of ice cover feedbacks. *Glob. Planet. Change* **75** (3), 155–172.

Mockler, E. M., Chun, K. P., Sapriza-Azuri, G., Bruen, M. & Wheater, H. S. 2016 Assessing the relative importance of parameter and forcing uncertainty and their interactions in conceptual hydrological model simulations. *Adv. Water Resour.* **97**, 299–313.

Nash, J. E. & Sutcliffe, J. V. 1970 River flow forecasting through conceptual models part I – A discussion of principles. *J. Hydrol.* **10** (3), 282–290.

Nijssen, B., O'Donnell, G. M., Hamlet, A. F. & Lettenmaier, D. P. 2001 Hydrologic sensitivity of global rivers to climate change. *Clim. Change* **50** (1–2), 143–175.

Nobrega, M. T., Collischonn, W., Tucci, C. E. M. & Paz, A. R. 2011 Uncertainty in climate change impacts on water resources in the Rio Grande Basin, Brazil. *Hydrol. Earth Syst. Sci.* **15** (2), 585–595.

Pedhazur, E. J. & Schmelkin, L. P. 2013 *Measurement, Design, and Analysis: An Integrated Approach*. Psychology Press, New York.

Pourmokhtarian, A., Driscoll, C. T., Campbell, J. L., Hayhoe, K., Stoner, A. M., Adams, M. B., Burns, D., Mitchell, M. J. & Shanley, J. B. 2017 Modeled ecohydrological responses to climate change at seven small watersheds in the northeastern United States. *Glob. Change Biol.* **23** (2), 840–856.

Qin, Y., Yang, D., Gao, B., Wang, T., Chen, J., Chen, Y., Wang, Y. & Zheng, G. 2017 Impacts of climate warming on the frozen ground and eco-hydrology in the Yellow River source region, China. *Sci. Total Environ.* **605**, 830–841.

Ramirez-Villegas, J. & Jarvis, A. 2010 Downscaling global circulation model outputs: the delta method decision and policy analysis Working Paper No. 1. *Pol. Anal.* **1**, 1–18.

Rasouli, K., Pomeroy, J. W., Janowicz, J. R., Carey, S. K. & Williams, T. J. 2014 Hydrological sensitivity of a northern mountain basin to climate change. *Hydrol. Process.* **28** (14), 4191–4208.

Ren, D., Xu, X., Hao, Y. & Huang, G. 2016 Modeling and assessing field irrigation water use in a canal system of Hetao, upper Yellow River basin: application to maize, sunflower and watermelon. *J. Hydrol.* **532**, 122–139.

Schaake, J. C. 1990 *From Climate to Flow. Climate Change and US Water Resources*. John Wiley & Sons Inc., New York, pp. 177–206.

Shen, M., Chen, J., Zhuan, M., Chen, H., Xu, C. Y. & Xiong, L. 2018 Estimating uncertainty and its temporal variation related to global climate models in quantifying climate change impacts on hydrology. *J. Hydrol.* **556**, 10–24.

Singh, S. K., Ibbitt, R., Srinivasan, M. S. & Shankar, U. 2017 Inter-comparison of experimental catchment data and hydrological modelling. *J. Hydrol.* **550**, 1–11.

Smelser, N. J. & Baltes, P. B. (eds) 2001 *International Encyclopedia of the Social and Behavioral Sciences*. Elsevier, Amsterdam.

Srivastava, P. K., Han, D., Rico-Ramirez, M. A. & Islam, T. (2014) Sensitivity and uncertainty analysis of mesoscale model downscaled hydro-meteorological variables for discharge prediction. *Hydrol. Process.* **28** (15), 4419–4432.

Tang, C., Crosby, B. T., Wheaton, J. M. & Piechota, T. C. 2012 Assessing streamflow sensitivity to temperature increases in the Salmon River Basin, Idaho. *Glob. Planet. Change* **88**, 32–44.

Tatsumi, K. & Yamashiki, Y. 2015 Effect of irrigation water withdrawals on water and energy balance in the Mekong River Basin using an improved VIC land surface model with fewer calibration parameters. *Agric. Water Manage.* **159**, 92–106.

Teklesadik, A. D., Alemayehu, T., van Griensven, A., van Griensven, A., Kumar, R., Liersch, S., Eisner, S., Tecklenburg, J., Ewunte, S. & Wang, X. 2017 Inter-model comparison of hydrological impacts of climate change on the Upper Blue Nile basin using ensemble of hydrological models and global climate models. *Clim. Change* **141** (3), 517–532.

Teutschbein, C., Wetterhall, F. & Seibert, J. 2011 Evaluation of different downscaling techniques for hydrological climate-change impact studies at the catchment scale. *Clim. Dyn.* **37** (9–10), 2087–2105.

Trudel, M., Doucet-Généreux, P. L. & Leconte, R. 2017 Assessing river low-flow uncertainties related to hydrological model calibration and structure under climate change conditions. *Climate* **5** (1), 19.

Wang, T., Yang, H., Yang, D., Qin, Y. & Wang, Y. 2018 Quantifying the streamflow response to frozen ground degradation in the source region of the Yellow River within the Budyko framework. *J. Hydrol.* **558**, 301–313.

Xu, Z. X., Zhao, F. F. & Li, J. Y. 2009 Response of streamflow to climate change in the headwater catchment of the Yellow River basin. *Quat. Int.* **208** (1–2), 62–75.

Yang, H. & Yang, D. 2011 Derivation of climate elasticity of runoff to assess the effects of climate change on annual runoff. *Water Resour. Res.* **47** (7), 197–203.

Yang, J., Ding, Y. & Chen, R. 2007 Climatic causes of ecological and environmental variations in the source regions of the Yangtze and Yellow Rivers of China. *Environ. Geol.* **53** (1), 113–121.

Yuan, F., Zhao, C., Jiang, Y., Ren, L., Shan, H., Zhang, L., Zhu, Y., Chen, T., Jiang, S., Yang, X. & Shen, H. 2017 Evaluation on uncertainty sources in projecting hydrological changes over the Xijiang River basin in South China. *J. Hydrol.* **554**, 434–450.

Zarch, M. A. A., Sivakumar, B., Malekinezhad, H. & Sharma, A. 2017 Future aridity under conditions of global climate change. *J. Hydrol.* **554**, 451–469.

Zhai, R. & Tao, F. 2017 Contributions of climate change and human activities to runoff change in seven typical catchments across China. *Sci. Total Environ.* **605**, 219–229.

Zhang, X., Tang, Q., Zhang, X. & Lettenmaier, D. P. 2014 Runoff sensitivity to global mean temperature change in the CMIP5 models. *Geophys. Res. Lett.* **41** (15), 5492–5498.

Zhang, Q., Liu, J., Singh, V. P., Shi, P. & Sun, P. 2017 Hydrological responses to climatic changes in the Yellow River basin, China: climatic elasticity and streamflow prediction. *J. Hydrol.* **554**, 635–645.

Zhou, D. G. & Huang, R. H. 2012 Response of water budget to recent climatic changes in the source region of the Yellow River. *Chin. Sci. Bull.* **57** (17), 2155–2162.

First received 4 December 2017; accepted in revised form 3 June 2018. Available online 5 July 2018